Developmental Biology 353 (2011) 194–205

Contents lists available at ScienceDirect

Developmental Biology

journal homepage: www.elsevier.com/developmentalbiology

Shh signalling restricts the expression of *Gcm2* and controls the position of the developing parathyroids

Armelle Grevellec [a], Anthony Graham [b], Abigail S. Tucker [a,*]

[a] King's College London, Department of Craniofacial Development and Orthodontics, Floor 27 Guy's Tower, Guy's Hospital, London Bridge, London SE1 9RT, UK
[b] King's College London, MRC Centre for Developmental Neurobiology, 4th Floor New Hunt's House, Guy's Hospital, London Bridge, London SE1 9RT, UK

ARTICLE INFO

Article history:
Received for publication 20 September 2010
Revised 12 February 2011
Accepted 14 February 2011
Available online 22 February 2011

Keywords:
Parathyroid
Gcm2
Shh
Pharyngeal pouch

ABSTRACT

The parathyroid glands originate from the endoderm of the caudal pharyngeal pouches. How these parathyroids are restricted to developing in the caudal pouches is unclear. In this paper we investigate the role of *Shh* signalling in patterning the vertebrate pharyngeal pouches, and show that Hh signalling may be involved in restricting the expression of the parathyroid marker *Gcm2* in the pharyngeal epithelium. In the chick and mouse, *Shh* signalling is excluded or highly reduced in the posterior/caudal pouches, where the parathyroid marker *Gcm2* is expressed, while remaining at high levels in the more anterior pouches. Moreover, though the block of *Shh* signalling at early developmental stages results in the loss of chick *Gcm2* expression, at later stages, it induces ectopic *Gcm2* expression domains in the second and first pharyngeal epithelium, suggesting that HH signalling prevents *Gcm2* in those tissues. These ectopic domains go on to express other parathyroid markers but do not migrate and develop into ectopic parathyroids. Differences in the expression of *Gcm2* in the chick, mouse and zebrafish, correlate with changing patterns of *Shh* signalling, indicating a conserved regulatory mechanism that acts to define pouch derivatives.

Introduction

The developing face and neck arise from the pharyngeal arches, a series of bulges that form either side of the developing head. The arches comprise a core mesoderm enclosed in neural crest tissue, and are surrounded externally by ectoderm and internally by endoderm. During development, the endoderm and ectoderm invaginate towards each other delineating the arches and forming, in between, a separating membrane consisting of an endodermal pouch on the inside and ectodermal cleft on the outside. As well as physically defining the pharyngeal region, the clefts and pouches also form important structures, such as the ear-drums, parathyroids, tonsils, thymus and ultimobranchial bodies (reviewed by Grevellec and Tucker, 2010). Each pouch/cleft gives rise to a specific organ, although this can vary considerably between different species.

The parathyroids develop from the caudal pouches, with two sets of parathyroids developing from the third and fourth pouches in humans and birds, while only one set forms from the third pouch in rodents. The parathyroids are endocrine glands unique to tetrapods that secrete a peptidic hormone essential for the regulation of calcium and phosphate homeostasis named parathyroid hormone (*PTH*) (Potts, 2005). The parathyroids can be detected early on in their development by the expression of *Gcm2* that turns on at E9.5 in the mouse and HH20 in the chick (Gordon et al., 2001; Okabe and Graham, 2004). *Gcm2* has been shown to be an excellent marker of the early parathyroid, coming on in the anterior third pouch before other classic parathyroid markers, such as *PTH* and *CasR* (Gordon et al., 2001; Liu et al., 2007). In keeping with the restricted origin of the parathyroids, in the mouse, *Gcm2* expression is only observed in the developing third pouch, while in the chick, expression is observed in the third and fourth pouches with transient expression also being observed in the second pouch (Okabe and Graham, 2004).

Unlike the terrestrial vertebrates, fish do not develop parathyroids. Still, they display *Gcm2* expression in the arches. Indeed, in the zebrafish, *Gcm2* is progressively activated in the epithelium of the third to seventh pharyngeal arches from 32- to 72 hpf. It is transiently expressed in a portion of the first and second arches from 40- to 48 hpf. Later in development, *Gcm2* remains evident in the gill epithelium until at least E5 (Chang et al., 2009; Hanaoka et al., 2004; Hogan et al., 2004; Okabe and Graham, 2004). The expression of *Gcm2* in the pharyngeal arch epithelium and the gill buds, which are derived from this region, has led to the hypothesis that the gills are evolutionarily related to the tetrapod parathyroid gland (Okabe and Graham, 2004). Indeed, the *Gcm2*-expressing internal gill buds also express *PTH* and *CasR* and are therefore likely to contribute to the regulation of extracellular calcium (Okabe and Graham, 2004).

Various signalling molecules and transcription factors have been linked to the development of the pouch derivatives, with loss of expression leading to defects in initiation, size and migration (Grevellec and Tucker, 2010). The signals important in initially defining what organ

* Corresponding author. Fax: +44 2071881674.
E-mail address: Abigail.tucker@kcl.ac.uk (A.S. Tucker).

0012-1606/$ – see front matter © 2011 Elsevier Inc. All rights reserved.
doi:10.1016/j.ydbio.2011.02.012

forms from which primordium, however, are unclear. A number of studies in mouse have demonstrated the presence of the Hh pathway genes *Shh* and *Ptc1* in the developing pharyngeal apparatus (Echelard et al., 1993; Goodrich et al., 1996; Hahn et al., 1996; Moore-Scott and Manley, 2005; Platt et al., 1997; Washington Smoak et al., 2005). *Ptc1* is induced by *Shh* signalling and is an excellent read out of *Shh* signalling. In the mouse embryo from E9.5 to E12.5, both *Shh* and *Ptc1* are spatially and temporally differentially activated within the pharyngeal region, with the anterior arches and pouches being subjected to higher Hh signalling than the posterior arches and pouches (Moore-Scott and Manley, 2005). This graded expression of *Shh* signalling has been suggested to play a role in providing the patterning information for the pouches, defining them into anterior domains with high *Shh* activity, and posterior/caudal domains with low or no *Shh* activity (Moore-Scott and Manley, 2005). Loss of *Shh* in the null mouse, leads to defects in the formation of all the arches and pouches, with loss of expression of *Gcm2*, indicating that *Shh* plays an important positive role in patterning the anterior and caudal pouches. We wished to investigate the relationship of *Shh* and parathyroid development, looking at the timing of *Shh* signalling during development of the caudal pouches in order to understand its relationship to the parathyroid marker *Gcm2,* and its role in restricting the development of the parathyroids to the caudal pouches.

Materials and methods

Collection of chicken embryos

Fertilised leghorn hen's eggs were incubated for up to 10 days at 38 °C in a humidified atmosphere. Embryo staging was determined referring to the normal stages of chicken development series of Hamburger and Hamilton (1992). At the required stage, embryos were removed from the eggs and the extra-embryonic membranes removed. Then, the embryos were fixed overnight at 4 °C in freshly prepared 4% paraformaldehyde (PFA).

Collection of mouse embryos

Pregnant CD1 mice were sacrificed by cervical dislocation. Noon on the day of discovery of the vaginal plug was designated E(embryonic day) 0.5. Embryos were harvested, decapitated and fixed overnight at 4 °C in freshly prepared 4% paraformaldehyde (PFA).

Collection of zebrafish embryos

24 hpf wild-type zebrafish embryos were raised until the desired stages at 28.5 °C in 35 mm Petri dishes filled up with E3 medium (5 mM NaCl, 0.17 mM KCl, 0.33 mM CaCl 2, and 0.33 mM MgSO4). No methylene blue was added to the medium as this antifungal solution was reported to cause autofluoresence when analysing the embryos by whole mount fluorescent ISH (Welten et al., 2006). Each Petri dish contained about 25 embryos and the medium was replaced every day. At 72 hpf, the embryos were placed onto cold-iced water for immobilisation and fixed in 4% PFA.

In-ovo cyclopamine injection

Cyclopamine (Sigma) was prepared in 45% 2-hydroxypropyl-B-cyclodextrin (Sigma) and diluted in PBS at a concentration of 2.43 M. At the desired stage, 15 μL to 30 μL of cyclopamine depending on the age of the embryo was administered as described by Cordero et al. (2004). Control embryos received a solution of 2-hydroxypropyl-B-cyclodextrin in PBS injected in a similar manner. After manipulation, the shell opening was sealed and the eggs were returned into the incubator. The embryos were left to develop up to E10 before further fixing.

Paraffin wax tissue sectioning

Following fixation in 4% paraformaldehyde at 4 °C, wildtype and experimental embryos were dehydrated through an ethanol series and embedded in paraffin wax. Eight-micrometre sections were cut and serially laid out over four superfrost plus slides. Sections from the E10 embryos were stained using a trichrome stain (haemotoxylin, alcian blue, and sirrus red).

In-situ hybridisation on whole-mount and paraffin wax sections of chick and mouse embryos

In situ hybridisation on chick embryonic tissues were carried out using the following DIG-labelled anti-sense riboprobes: *Gcm2*, linearised with *Nco1* and transcribed with Sp6, *Shh*, linearised with *Sal1* and transcribed with Sp6; *Ptc1*, linearised with *Sal1* and transcribed with T3; *FgF8*, linearised with *BamH1* and transcribed with T7; *Bmp4*, linearised with *BamH1* and transcribed with T3; *Pax1*, linearised with *XbaI* and transcribed with T3; *Eya1*, linearised with *Not1* and transcribed with T3; and *CasR*, linearised with *Sal1* and transcribed with T7. *PTH* expression was detected using a mixture of *PTH*-3′ and *PTH*-5′ antisenses riboprobes. *PTH*-3′ was linearised with *Sal1* and transcribed with T7; while *PTH*-5′ was linearised with *Nco1* and transcribed with Sp6. For the mouse tissue *Ptc1* was linearised with *BamH1* and transcribed with T3, while *Gcm2* was linearised with *Nco1* and transcribed with Sp6. Whole mount in situ hybridisations were performed as described previously (Mootoosamy and Dietrich, 2002). For in-situ hybridisation on wax sections, the sections were deparaffinised with Histoclear (Histo-Clear II, National Diagnostics) and rehydrated through an ethanol series. Then, they were treated with Proteinase K (20 μg/mL for 15 min), fixed for 20 min with PFA, and placed at 65 °C in a humidified chamber for overnight hybridisation with the DIG-labelled riboprobes diluted in 50% formamide, 5 mM EDTA, pH 8; 25 μg/mL heparin; 2% Tween20; 1.28X SSC; and 0.05 mg/mL yeast RNA. The following day, the slides were washed once in 2X SSC, 50% formamide, 0.1% Tween 20, and twice in 1X SSC for 30 min at 65 °C. They were then taken through three 30 min washes at RT in MABT (0.15 M NaCl, and 0.1 M maleic Acid; 0.1% tween), before blocking for 2 h in 10% goat serum (Sigma), and overnight incubation at 4 °C with the anti-DIG Fab fragment alkaline phosphatase conjugate antibody (Roche Diagnostics) (1:1000). Subsequently, the unbound antibodies were cleared off by four MABT washes, and a diluted staining solution of NBT/BCIP (Roche Diagnostics) was applied onto the tissues until a colour develops. The reaction was stopped with PBT, and the sections were dehydrated through an ascendant ethanol series. Previous to mounting, the tissues were lightly counterstained in pink by eosin.

Double fluorescent in-situ hybridisation on whole-mount zebrafish embryos

The steps of preparation of the embryos, hybridisation, post-hybridisation washes, and post-antibody washes were performed as described in Clay and Ramakrishnan (2005). The antibody detection of the labelled probes was carried out using the TSA-Plus Fluorescent System (Perkin Elmer Life Science) following the protocol detailed in Denkers et al. (2004). *Gcm2* was linearised by *Sal1* and transcribed by T7; *Ptc1* was linearised by *BamH1* and transcribed by T3.

Results

Shh signalling is excluded from, or reduced in, the Gcm2 expression

Differential expression of *Shh* and *Ptc1* within the pharyngeal pouches of the different arches has previously been observed in the mouse at E10.5 and E11.5 (Moore-Scott and Manley, 2005). To

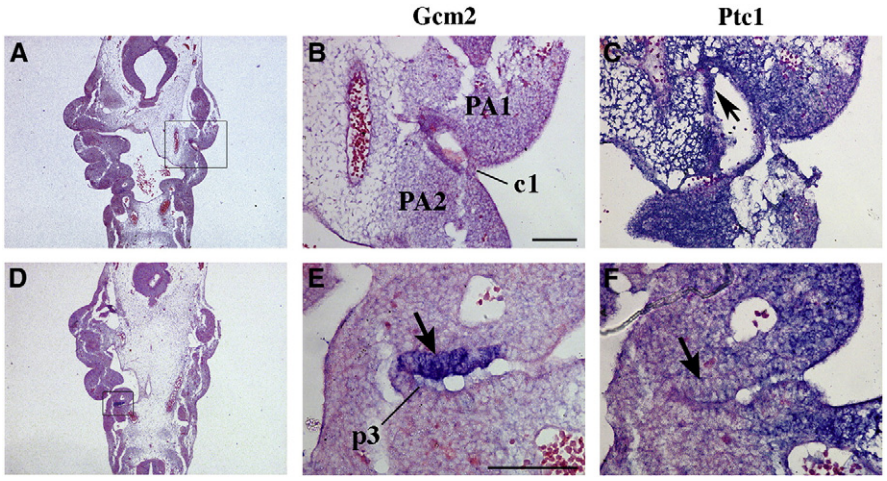

Fig. 1. Expression analysis of *Gcm2* and *Ptc1* in the mouse pharyngeal epithelium at E10.5. (A and B): No *Gcm2* is detected in the mouse' first cleft area (c1). (C): In contrast, the first cleft ectoderm strongly expresses *Ptc1* (arrow). (D, E): *Gcm2* labels the anterior part of the third pouch (p3) endoderm (arrow). (F): On serial section, this tissue shows reduced *Ptc1* expression (arrow). (A and B) are frontal sections. PA = pharyngeal arch. Scale-bars represent 200 μm.

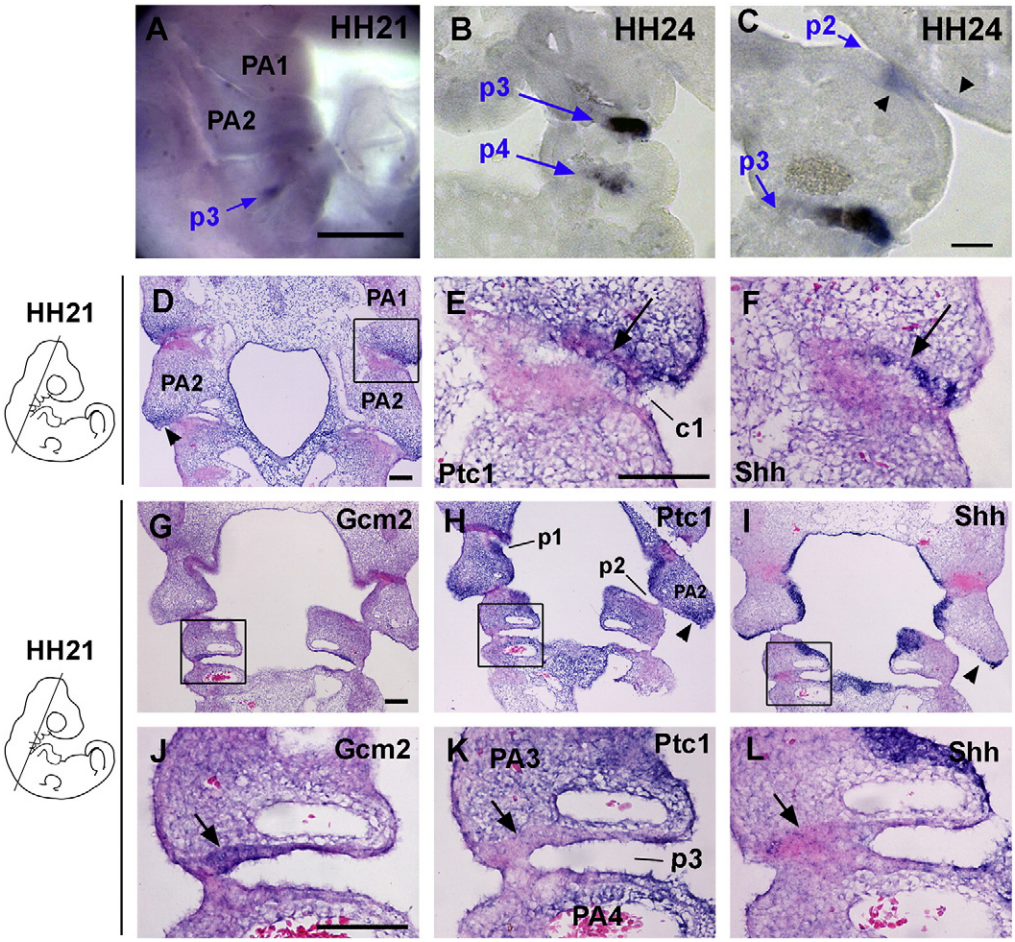

Fig. 2. Expression analysis of *Gcm2, Ptc1* and *Shh* in the chick pharyngeal pouch area at HH21–24. (A): At HH21, *Gcm2* is detected in the third pouch (p3). (B): At HH24, it is also seen in the fourth pouch (p4). On frontal sections, *Gcm2* is visible in the anterior endodermal portion of the third and fourth pouches (p3 and p4 arrows). (C):At a more ventral level, additional faint *Gcm2* labels the lateral posterior second arch and anterior third arch epithelium (arrowheads). (D and E): *Ptc1* is expressed in the anterior half of the first cleft ectoderm (arrow) as well as in the surrounding lateral mesenchyme of the posterior first arch. (F): On a serial section *Shh* is co-expressed with *Ptc1* in the cleft ectoderm (arrow). (G): *Gcm2* is present in the third pouch, whereas it is not detected in the first and second pouches and cleft epithelium. (H and I): On serial sections, *Ptc1* (H) and *Shh* (I) appear prominent in the posterior ectodermal margin of the second arch (arrowheads). *Ptc1* but not *Shh* is expressed in the first and second pouches (p1 and p2). (J): In the anterior third pouch, the presumptive parathyroid domain is marked by the presence of *Gcm2* (arrow). (K): On a serial section, *Ptc1* is present in the third and fourth arch mesenchyme and medial endoderm, but is restricted from the *Gcm2*-expressing pouch endoderm (arrow), as well as from the posterior part of the third pouch. (L): On a serial section, *Shh* is expressed in the medial arch endoderm, but is absent from the entire third pouch endoderm. The scale-bars correspond to 500 μm in (A), and 100 μm in the other panels. The boxes in (D and G–I) show the region highlighted in (E and F) and (J–L) respectively. The diagrams on the left show the plane and orientation of the sections in (D–L). PA = pharyngeal arch and c = pharyngeal cleft.

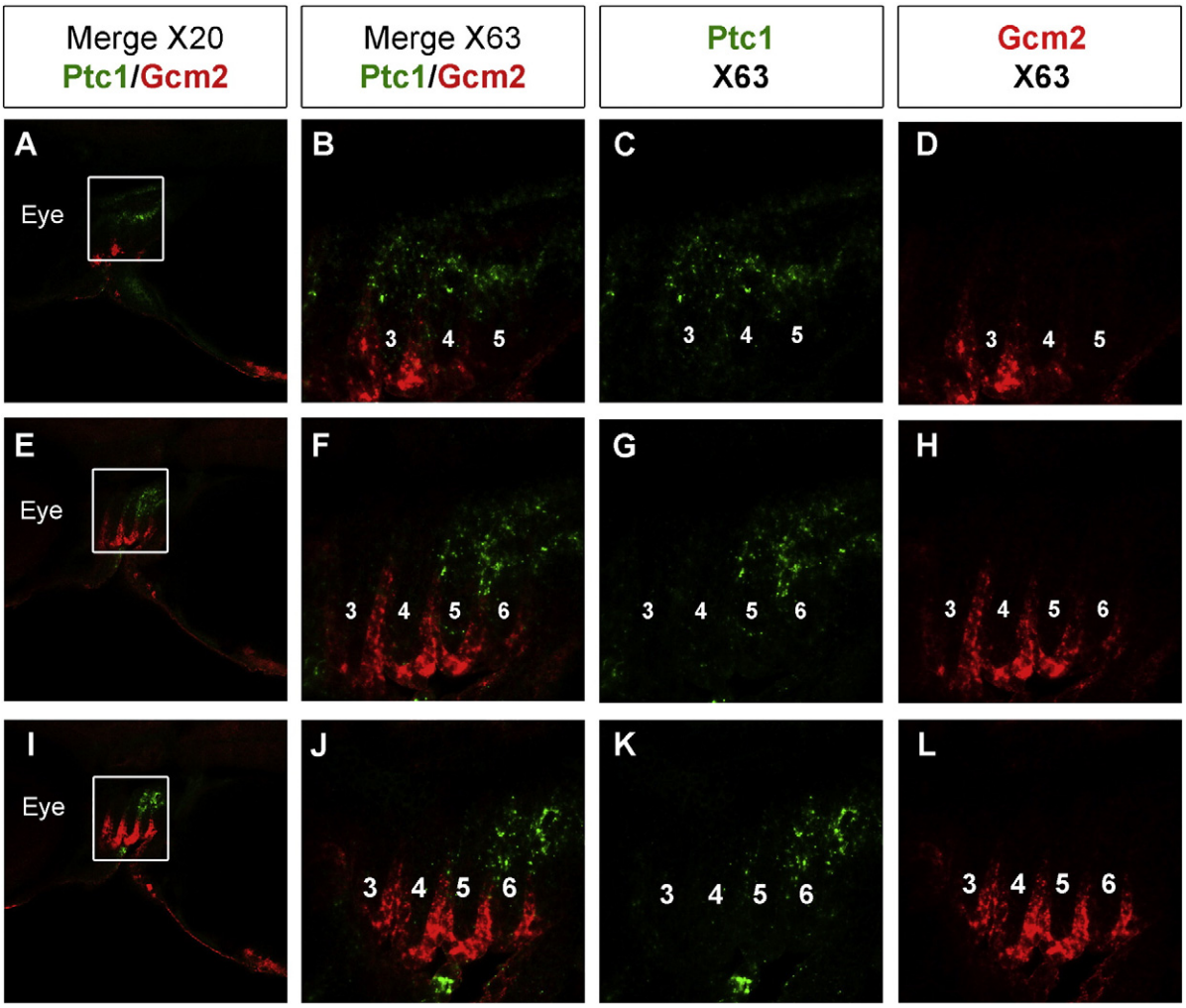

Fig. 3. Expression of *Gcm2* and *Ptc1* at 3 dpf in the zebrafish pharyngeal pouch region. Confocal analysis in the head region of a 3 dpf zebrafish embryo subjected to double whole-mount ISH for *Gcm2* (red) and *Ptc1* (green). (A, E and I): Merged images of *Ptc1* and *Gcm2* at distinct medio-lateral levels of the same embryos. (B, F and J): View at higher magnification (×63) of the arch area squared in the panels (A), (E) and (I) respectively. The numbers indicate the name of the pharyngeal arches. (C, G and K): *Ptc1* labels the entire pouch endoderm. (D, H and L): *Gcm2* labels the arch epithelium.

investigate this further we used serial sections to compare the expression of *Ptc1* with *Gcm2* at E10.5, when the endoderm pouches are clear. As previously shown, *Ptc1* was found at high levels in the rostral pouches, where there is no *Gcm2* expression, while in the *Gcm2* positive third pouch expression of *Ptc1* was at much lower levels, in the region where *Gcm2* was expressed (Fig. 1). To test whether this reduction of *Shh* signalling in the *Gcm2* expressing caudal pouches was also observed in other species with different patterns of *Gcm2* expression, we turned to the chick and zebrafish that have very different expression patterns of *Gcm2* during pharyngeal arch development.

In the chick, *Gcm2* was first detected in the third pharyngeal pouch at HH21 (Fig. 2A). By HH23–24, expression increased in the third pouch, and was initiated in the fourth pouch, in the dorsal anterior portion of the endodermal outpocketings (Fig. 2B). In addition *Gcm2* was faintly transcribed in a limited domain of the caudal second arch and rostral third arch epithelium in a few embryos (Fig. 2C, arrowheads, 3/7 embryo). This second arch expression domain was transient, with only 2 out of 24 embryos retaining *Gcm2* expression in the second pouch by HH26.

In the rostral arches, *Shh* was expressed in a restricted fashion throughout the medial pharyngeal endoderm, as well as in the external anterior part of the first cleft (Fig. 2F), and in the posterior margin of the second arch (arrowhead Fig. 2I). Meanwhile, *Ptc1* colocalised with *Shh* in the first and second clefts, as well as in the pharyngeal medial endoderm (Fig. 2D, E, and H). In addition, it was present throughout the first and second arch mesenchyme, as well as in the first and second pouches, with strong expression levels in the areas surrounding the *Shh* transcripts (Fig. 2H and I). In the caudal pharyngeal region, *Ptc1* expression was prominent in the medial aspect of the third and fourth arch mesenchyme (Fig. 2H and K).

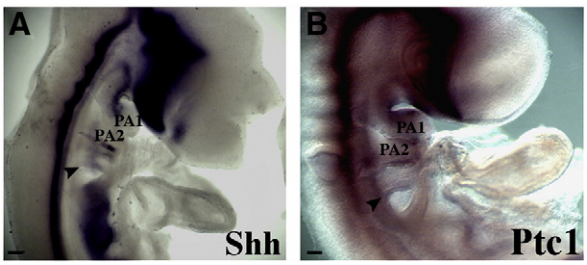

Fig. 4. Early expression of *Shh* and *Ptc1* in the chick pharyngeal arches. Whole-mount ISH for *Shh* and *Ptc1* on wild-type embryos at HH16. (A): *Shh* is expressed in the foregut endoderm as well as in the second pouch epithelium. (B): *Ptc1* is present in the oral ectoderm and mesenchyme as well as in the posterior aspect of each developing arch. Arrows indicate the third pouch.

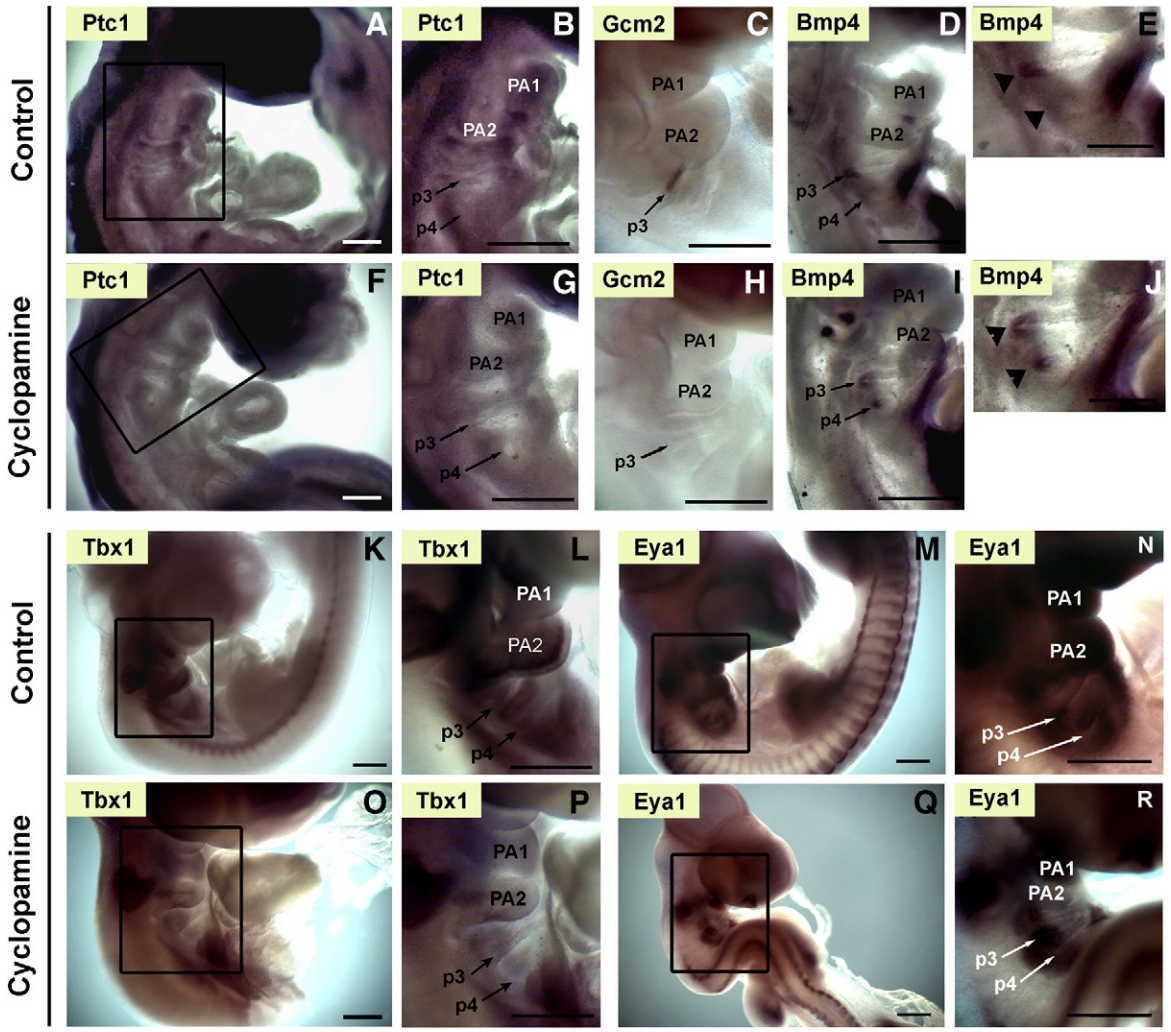

Fig. 5. Effect of in-ovo cyclopamine administration at HH16–17 on gene expression in the pouch area at HH21–23. Embryos treated with 15–20 μL of control HbC vehicle (A–E, K–N) or cyclopamine (F–J, O–R) at HH16–17 and analysed for gene expression in the pharyngeal region at HH21–23. (B and G), (L and N) and (P and R) show at higher magnification the zones squared in (A and F), (K and O) and (M and Q) respectively. (A–E): In the controls, *Ptc1* (A and B) is expressed throughout the pharyngeal arches; *Gcm2* (C) is expressed in the anterior part of the third pouch; and *Bmp4* (D and E) is expressed in the dorsal posterior aspect of the third pouch. (F–J): Following cyclopamine treatment, *Ptc1* (F and G) is significantly reduced in the arches; *Gcm2* (H) is reduced or abolished in the third pouch (p3) whereas *Bmp4* (I and J) appears upregulated in the fourth pouch (p4, arrow). (K–N): in the controls, *Tbx1* (K and L) is strongly expressed in the arch mesenchyme, and is also visible in the third and fourth pouches, while *Eya1* (M and N) is present throughout the arch mesenchyme and epithelium. (O–R): In the embryos exposed to cyclopamine *Tbx1* (O and P) is reduced in the arch mesenchyme and epithelium, including in the third and fourth pouches, while *Eya1* (M and N) appears decreased in the second arch as well as in the medial aspect of the third and fourth arch mesenchyme and epithelia. Scale bars represent 500 μm in (A, F, K, M, O and Q).

Finally, whereas *Shh* and *Ptc1* transcripts robustly labelled the caudal medial endoderm, they appeared excluded from the zone of the third pouch expressing *Gcm2* (Fig. 2G, J–L). Similar observations were made in the fourth pouch at HH24 (data not shown).

We also investigated the expression pattern of *Ptc2*, which in the chick, unlike the mouse, is responsive to Hh signalling. A similar exclusion of *Ptc2* from the caudal pouch endoderm was shown by *Ptc2* (data not shown).

Therefore, in the chick as in mouse, Hh pathway activity, evidenced by *Ptc1* and *Ptc2* expression, appears higher in the anterior than in the posterior arches. In addition, whereas it is present in the rostral pouches, it appears weak or absent in the third and fourth

Fig. 6. In-ovo cyclopamine administration at HH20 ectopically activates *Gcm2* expression in the first cleft and posterior second arch epithelium. Embryos treated with 30–50 μL of control HbC vehicle (D, J, P, and V) or cyclopamine (A, G, M, and S) at HH21 and analysed for *Ptc1* and *Gcm2* in the pharyngeal region by ISH at HH24 (A–R) or HH27–28 (S–Y). The squares in the left panels indicate the zones shown at higher magnification in the adjacent panels. (A–B): In the cyclopamine-treated embryos at HH24, *Ptc1* is weak in the first pouch (p1) and cleft (c1), including in the anterior part of the cleft (arrow). (C): On a serial section, *Gcm2* is present in the anterior aspect of the cleft ectoderm (arrow). (D–E): In the controls at HH24, *Ptc1* is evident in the anterior first pouch and cleft (arrow). (F): On an adjacent section, *Gcm2* is absent from these tissues (arrow). (G, H): Following Hh inhibition, *Ptc1* appears strongly downregulated at HH24 in a domain of the posterior second arch epithelium (H, arrow). (I): On an adjacent section, this domain shows prominent *Gcm2* expression (arrows). (J and K): In the controls at HH24, *Ptc1* is expressed at a high level throughout the caudal second arch margin, except in a limited area of the epithelium, which appears smaller than the one seen in the cyclopamine treated animals (compare H and K, arrows). (L): On a serial section, *Gcm2* is detected in the zone of the posterior second arch epithelium where *Ptc1* is absent (arrows). (M–R): In the third pouch of the controls (M–O) and cyclopamine-exposed embryos (P–R), virtually no *Ptc1* is detected (N and Q) whereas *Gcm2* is robust (arrows, O and R). (S and T): At HH27–28, reduced *Ptc1* is detected in the first cleft of the cyclopamine-treated embryos. (U): On a serial section, ectopic *Gcm2* is seen in the anterior first cleft ectoderm. (V–W): At HH27–28 the controls still display *Ptc1* in the anterior first cleft, even though expression levels seem reduced compared with HH24. (Y): On an adjacent section, no *Gcm2* is detected in the anterior first cleft. The diagrams on the left-hand side of the figure indicate the plane and orientation of the sections. The scale-bars in (A–H) stand for 100 μm. PA = pharyngeal arches.

endodermal outpocketings, particularly at the level of the presumptive parathyroid. Finally, interestingly, Hh pathway activity appeared especially concentrated in confined areas of the anterior first and second clefts.

Whereas, in mouse or avian embryos, early *Gcm2* expression is restricted to the anterior part of the caudal pouch endoderm, in fish it is primarily confined to the pharyngeal arch epithelium (Hogan et al., 2004; Okabe and Graham, 2004). In zebrafish, *Shh*, *Ptc1* and *Ptc2* transcripts have been reported in the gill area from 32 hpf to 72 hpf (Krauss et al., 1993; Lewis et al., 1999). We therefore wished to see whether *Gcm2* and *Ptc1* expressions in the zebrafish are also mutually exclusive in the developing pouches and clefts.

Our expression analysis reveals that at 72 hpf, *Ptc1* is present throughout the pharyngeal pouch endoderm up to the lateral tips of

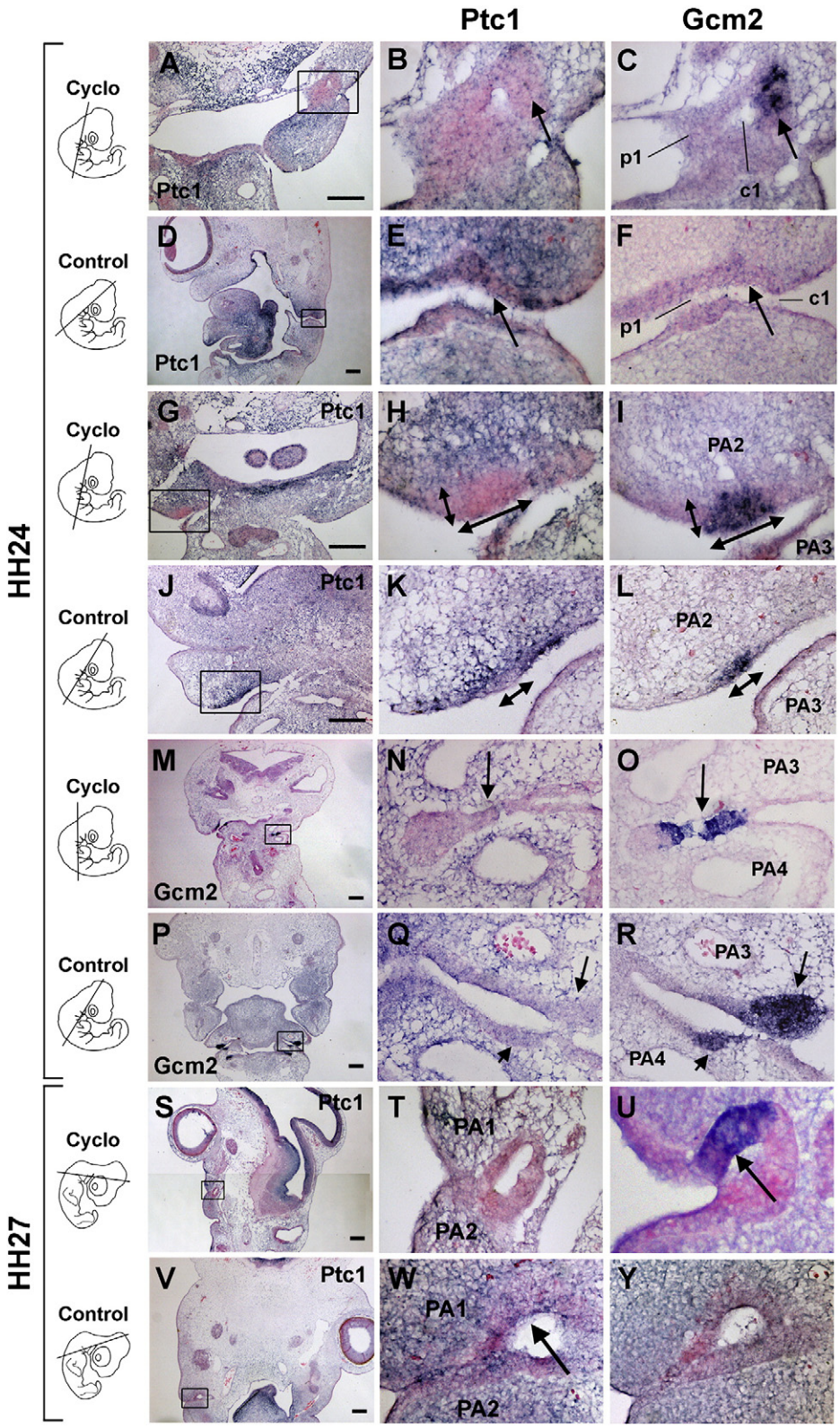

the endodermal out-pocketings. By contrast, it is absent from the gill epithelium, including the clefts (Fig. 3C, G, and K). *Gcm2* is excluded from the pharyngeal pouch endoderm, while it is prominent in the arch ectoderm, as well as in the ectodermal groove (Fig. 3D, H, and L). Overall, *Ptc1* and *Gcm2* expression appear strictly restricted from each other, with *Ptc1* expression marking the pharyngeal pouch, and *Gcm2* expression labelling the pharyngeal arch epithelium and the cleft (Fig. 3B, F, and J).

Gcm2 expression is therefore localised to regions with low or no *Shh* signalling in mouse, chick and zebrafish.

Early loss of Shh signalling in the chick mimics the Shh null mutant with loss of the parathyroid

Analysis of the *Shh* null mutant mouse has shown that patterning of the third pharyngeal pouch is dependent on *Shh* signalling (Moore-Scott and Manley, 2005). In the *Shh* knockout, the pattern of the pharyngeal pouches is disrupted and in the third pouch the *Gcm2* expression domain is lost while the neighbouring *Bmp4* expressing presumptive thymus domain expands. We therefore treated chick embryos *in ovo* with cyclopamine at HH14–16, before the onset of

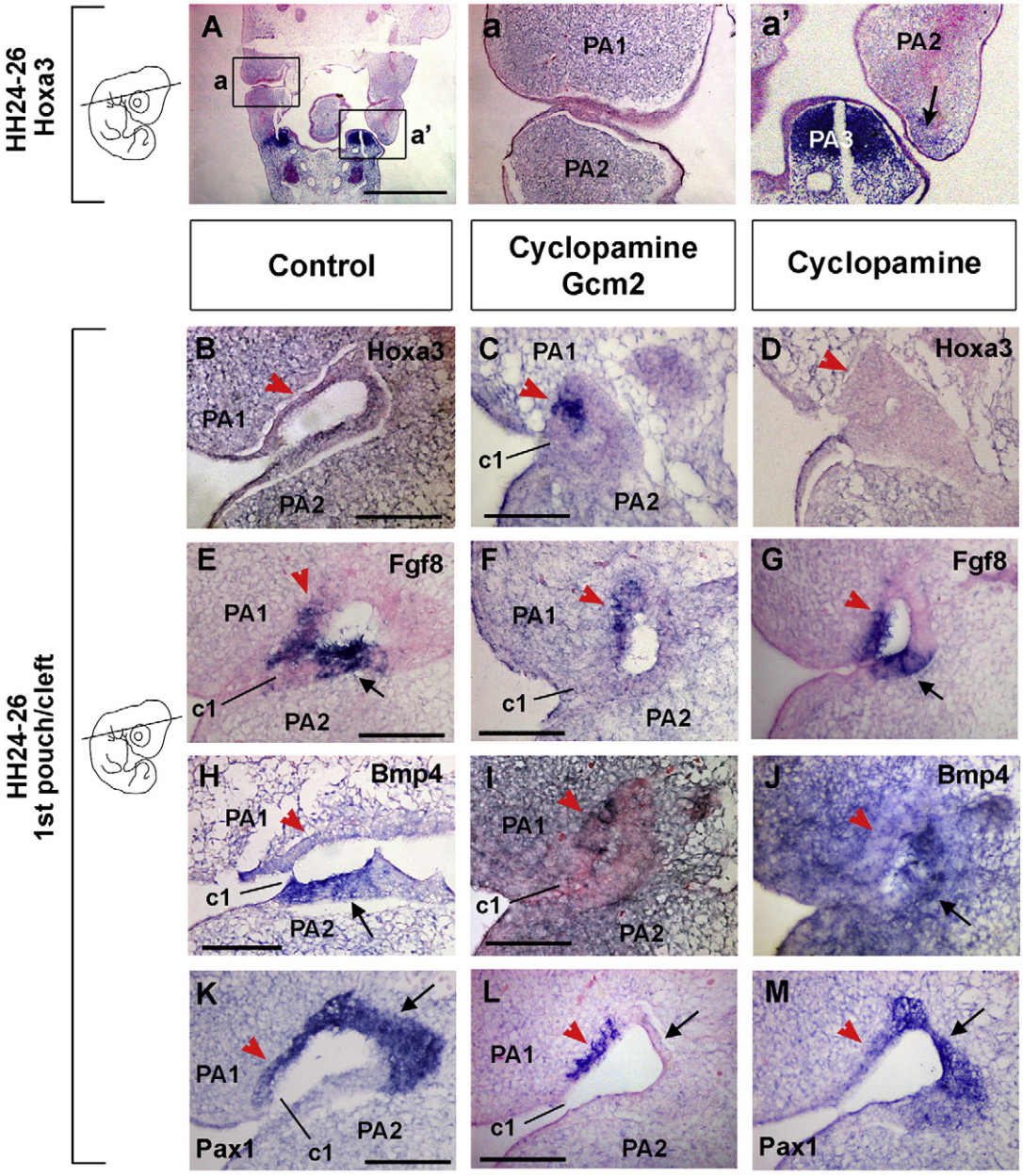

Fig. 7. Ectopic *Gcm2* expression overlaps with *Fgf8* and *Pax1* but not *Hoxa3* or *Bmp4* in the first cleft. (A, a and a'): At HH24 in the WTs, *Hoxa3* is expressed in the third and fourth arches (A) as well as the posterior aspect of the second arch epithelia (arrow, a'), whereas it is excluded from the first pouch and cleft. The squares in (A) indicates the areas shown at higher magnification in (a) and (a'). (B–M): Embryos treated with 30 μL of control HbC vehicle (B, E, H, and K) or cyclopamine (C, F, I, and L) at HH20–22 and analysed for gene expression in the first cleft at HH24–26. (C, F, I, and L) and (D, G, J, and M) are serial sections. (C, F, I, and L): Cyclopamine treatment leads to ectopic *Gcm2* activation in the anterior first cleft (red arrowheads). (B): The controls show absent *Hoxa3* expression in the first cleft. (D): Similarly, the cyclopamine-treated embryos display no *Hoxa3* in the first cleft. (E): In the controls, *Fgf8* is present in restricted domains of the anterior and posterior cleft (black arrow, E). (G): In the cyclopamine-exposed embryos, *Fgf8* appears unchanged; it partly overlaps with ectopic *Gcm2* (F, G, red arrowheads). (H): In the controls, *Bmp4* is expressed in the posterior part of the cleft (black arrow). (J): In the cyclopamine-treated embryos, such expression is unaffected. Ectopic *Gcm2* is excluded from the *Bmp4* domain (red arrowheads I, J). (K): In the controls, *Pax1* is evident in the anterior and distal portion of the cleft (black arrow). (M): *Pax1* is unchanged in the embryos exposed to cyclopamine; it partly overlaps with ectopic *Gcm2* (red arrowhead, L, M). The scale-bars represent 1000 μm in (A) and 200 μm in the other panels. The approximate plane and orientation of the sections are indicated on the diagram on the left. PA = pharyngeal arch; c = pharyngeal cleft; p = pharyngeal pouch.

Gcm2 expression. At this time-point *Shh* is expressed in the foregut endoderm and second pouch epithelium, with active *Shh* signalling, as indicated by *Ptc1* expression, located at the base of each developing arch (Fig. 4). After treatment with cyclopamine the embryos were left to develop until HH21–23. Confirming that the cyclopamine was functional in the embryos at this stage, *Ptc1* expression was clearly reduced in specimens subjected to the teratogen (Fig. 5A and F). This early treatment resulted in a failure of *Gcm2* expression to initiate and enhanced *Bmp4* expression in the caudal pouches, while all arches demonstrated a reduction in *Tbx1* and *Eya1*, two key transcription factors with roles in pharyngeal arch patterning, when analysed at HH21–23 (Fig. 5C–E, H–R). These experiments thus confirm that *Shh* plays an important role in patterning the pharyngeal arches at early stages of development. No change in *Hoxa3* gene expression was observed, indicating no change in the overall layout of the embryo (data not shown).

Later loss of Shh signalling leads to ectopic expression of Gcm2 in the anterior pouches

Despite this early positive role of *Shh* on pharyngeal arch patterning, and *Gcm2* expression, the exclusion of *Shh* signalling in the chick caudal pouch endoderm indicates that at later stages of pharyngeal pouch development *Shh* signalling may inhibit *Gcm2* expression. We therefore inhibited *Shh* signalling, using cyclopamine *in ovo*, but at later stages once the arch pattern is set up and *Gcm2* is induced in the third pouch. Specifically, we wished to test whether inhibition of *Shh* signalling would lead to an upregulation of parathyroid markers in the anterior pouches.

Relative to the controls, Hh inhibition at later stages (HH21) caused no apparent change in *Gcm2* transcription level in the third pouch (Fig. 6O and R, 8/8). It is possible that slight changes in expression occurred but could not be assessed by in situ. In the posterior second arch epithelial margin, where a transient *Gcm2* positive domain is observed in controls, application of cyclopamine increased the extent of *Gcm2* expression, with the area of expression being significantly larger and persisting longer in the cyclopamine-treated embryos compared to the controls (Fig. 6I and L) (N = 3/19 in controls and N = 21/29 cyclopamine treated). Moreover, in the anterior first ectodermal cleft, cyclopamine treatment induced a completely new *Gcm2* expression domain in 18/21 embryos (Fig. 6C), whereas expression of this gene in the first pouch/cleft was never evidenced in the controls (Fig. 6F, 0/15).

In the anterior first and second clefts and pouches of the controls, strong *Ptc1* was detected throughout the epithelium, except in the limited caudal second arch epithelial zone that occasionally expressed *Gcm2* (Fig. 6E and K, N = 4/4). By contrast, in the embryos exposed to cyclopamine, highly reduced *Ptc1* was observed in the ectopic *Gcm2* positive area of the first cleft and posterior second arch (Fig. 6B and H, N = 3/3). There is thus a clear correlation between loss of *Ptc1* and upregulation of *Gcm2*, in the lateral posterior first and second arch epithelia. The presence of active Hh signalling may therefore prevent the transcription of *Gcm2*.

Interestingly, subjecting the embryos to cyclopamine at HH24 similarly resulted in ectopic *Gcm2* activation in the rostral first ectodermal groove at HH27–28 (Fig. 6U and Y, 7/10). Again, this activation of *Gcm2* was correlated with a local diminution in *Ptc1* transcripts (Fig. 6T and W). Maintained *Shh* signalling in the anterior pouches from HH21 to 27 may therefore be necessary to repress the expression of *Gcm2*.

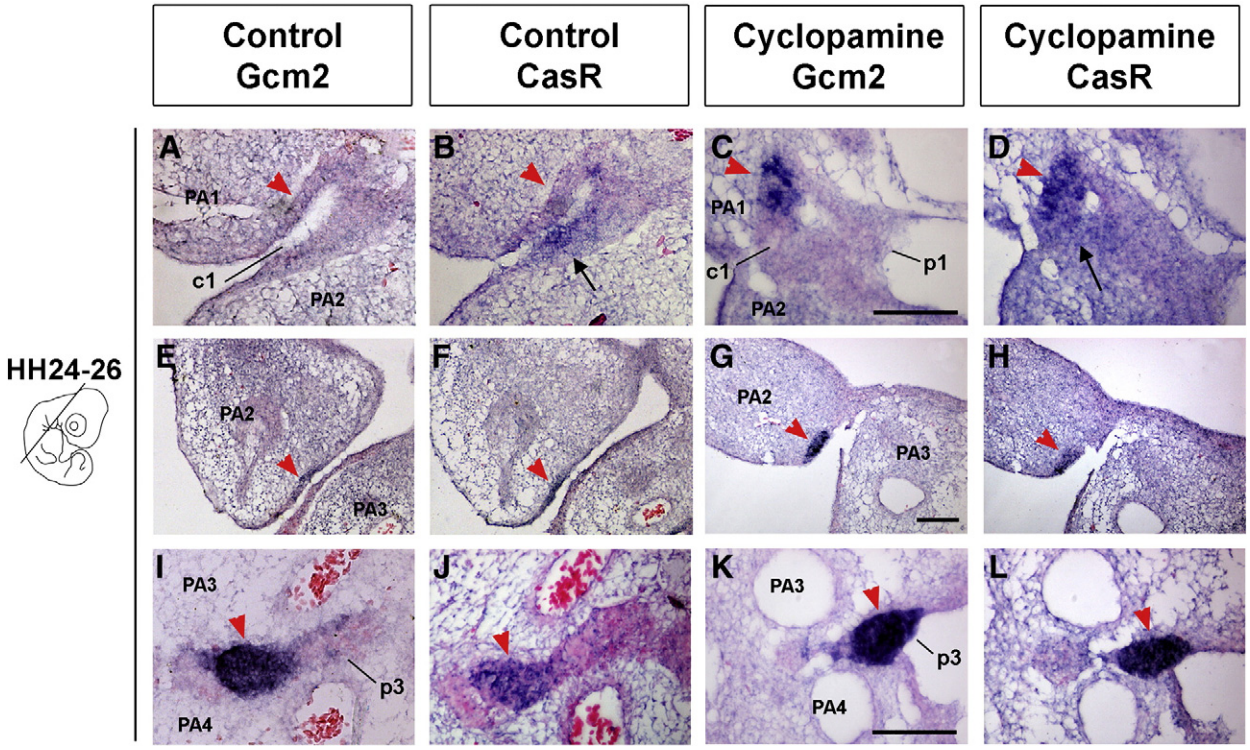

Fig. 8. *CasR* is upregulated in the cyclopamine-induced *Gcm2*-expressing domains. Embryos treated with 30 μL of control HbC vehicle (A, E, and I) or cyclopamine (C, G, and K) at HH20–22 and analysed for gene expression in the pouch and cleft regions at HH24–26. (A and B): In the controls, no *Gcm2* (A) is detected in the first cleft, while *CasR* (B) is evident in the posterior aspect of the ectodermal groove. (C): In the embryos treated with cyclopamine, ectopic *Gcm2* is seen in the anterior first cleft (red arrowhead). (D): On an adjacent section, *CasR* is visible in the posterior cleft (black arrow), but also in the anterior aspect of the latter, where it is co-expressed with *Gcm2* (red arrowhead). (E): In some controls, *Gcm2* is detected in the posterior second arch epithelial margin (red arrowhead). (F): On a serial section, *CasR* co-localises with this *Gcm2* expression (red arrowhead). (G): Cyclopamine treatment leads to *Gcm2* upregulation in the posterior second arch epithelium. (H): On an adjacent section, *CasR* expression is evident in the cyclopamine-induced *Gcm2* domain (red arrowhead). (I and J): *Gcm2* (I) and *CasR* (J) are co-expressed in the third pouch of the controls. (K and L): Similarly, *Gcm2* (K) and *CasR* (L) appear co-expressed in the third pouch of the cyclopamine-treated embryos (red arrowheads). Scale-bars represent 200 μm. The approximate plane and orientation of the sections are indicated on the diagram on the left hand side of the figure. PA = pharyngeal arch; c = pharyngeal cleft; p = pharyngeal pouch.

Correlation of Gcm2 expression with Hoxa3

In the mouse *Gcm2* is restricted to the third and fourth pouches, while in the chick a transient expression is also observed in the second arch. *Gcm2* expression is thought to be expressed downstream of *Hoxa3*, and in keeping with this *Gcm2* expression is lost in *Hoxa3* mutants (Su et al., 2001). In the mouse, the level of *Hoxa3* extends up to the third pharyngeal arch so that the third and fourth pouches are both *Hoxa3* positive, while the first and second pouches are *Hoxa3* negative (Hunt and Krumlauf, 1992; Manley and Capecchi, 1995, 1998; Manley et al., 2004). The other *Hox3* genes are expressed in the caudal arches but not in the pouches at this stage (Manley and Capecchi, 1998). A similar boundary of *Hoxa3* is observed in the chick at HH18 (Hunt et al., 1998). However, during later development in the chick (HH24–26), the level of *Hoxa3* extends more anteriorly up to and including the second pharyngeal pouch (Fig. 7A). The transient second arch expression domain of *Gcm2* overlaps with this later extended expression domain of *Hoxa3* (Fig. 7a and a'). The timing and position of the transient second pouch expression domain is therefore tightly linked with the expression of *Hoxa3*. Given this finding, we wished to assess whether the ectopic first arch expression domain of *Gcm2* induced after cyclopamine treatment was also linked with a change in the expression of *Hoxa3*. Embryos treated with cyclopamine at HH20–24 were selected for ectopic *Gcm2* activation in the first cleft. In the first cleft and caudal second arch epithelium of the cyclopamine-subjected embryos (5/5), *Hoxa3* expression was normal compared with the controls, implying that the ectopic *Gcm2* expression visible in these areas does not reflect a change in pharyngeal arch patterning (Fig. 7B, C, and D).

The ectopic *Gcm2* domain in the first pouch and cleft is restricted to the anterior half of the epithelium, and was not observed more posteriorly despite the lack of *Shh* signalling in this region (Fig. 6U and Y). This indicated that another factor might be restricting the expression of the ectopic *Gcm2*. In normal third pouch development the developing parathyroids are positively regulated by *Fgf8* and *Pax1* (Abu-Issa et al., 2002; Frank et al., 2002; Liu et al., 2007; Su et al., 2001; Vitelli et al., 2002; Wallin et al., 1996), and negatively regulated by *Bmp4*, expressed in the thymus domain (Patel et al., 2006; Gordon et al., 2010). Interestingly, *Bmp4* is also expressed in the posterior domain of the first pharyngeal pouch and is excluded from the more anterior region (Fig. 7H). In the cyclopamine treated embryos, the ectopic *Gcm2* expression was located in the anterior domain and did not extend into the *Bmp4* region (Fig. 7I and J). *Fgf8* and *Pax1* transcripts were expressed in the first pouch/cleft epithelium in control embryos in both the anterior and posterior domain, but the expression overlapped only in a part of the anterior region (Fig. 7E and K). In cyclopamine treated embryos the ectopic *Gcm2* expression was found to overlap with these two factors, indicating that these two genes may be required for *Gcm2* expression (Fig. 7F, G, L, and M). In each case the expression of *Bmp4*, *Pax1* and *Fgf8* in the pharyngeal epithelium was not affected by the cyclopamine treatment (N = 5/5).

Loss of Shh signalling leads to ectopic expression of CasR but not PTH

In order to determine whether other parathyroid-specific genes may be ectopically activated in the anterior first cleft and/or posterior second arch epithelium following cyclopamine treatment, Hh-depleted embryos were analysed for *CasR* and *PTH* (*parathyroid hormone*) expression (Fig. 8 and Fig. S1). In the controls, *CasR* was co-expressed with *Gcm2* in the third pouch (Fig. 8I and J, 5/5). Expression of *CasR* was also observed in the second pouch in those embryos that showed *Gcm2* expression in this area (Fig. 8E and F 1/8). In addition, *CasR* was apparent in the caudal portion of the first cleft (Fig. 8B, 5/5), a region not associated with *Gcm2* or parathyroid development. Interestingly, after inhibition of *Shh* signalling, *CasR* was upregulated with ectopic *Gcm2* in the rostral first cleft (Fig. 8C and D, N = 3/5), and in the expanded *Gcm2* expression domain in the posterior second arch epithelium (Fig. 8G and H N = 3/5). The co-expression of *Gcm2* and *CasR*, two parathyroid markers, indicates that the first and second cleft regions had been transformed to a parathyroid fate. As *CasR* expression does not correlate specifically with *Gcm2*, we also investigated the expression of *PTH*. *PTH* is expressed later than *Gcm2* and *CasR* in the chick, once the parathyroids are already morphologically defined and have started to migrate. At HH26 no expression of *PTH* was observed (data not shown). From HH28 onwards *PTH* was expressed clearly in the third and fourth pouches, with no expression in the more rostral pouches (Fig. S1B and H). After treatment with cyclopamine no evidence of *PTH* in the first or second pouch/cleft epithelium was observed, despite strong ectopic expression of *Gcm2* (Fig. S1E and F N = 0/9). This would imply that loss of *Shh* signalling is not enough to create ectopic, functional parathyroids.

Ectopic Gcm2/CasR domains do not form ectopic parathyroids

In order to investigate whether ectopic parathyroids developed in our cyclopamine treated embryos, and to assess the consequence of *Gcm2*/*CasR* ectopic expression on the normal development of the first cleft, we treated embryos with cyclopamine at late stages as before

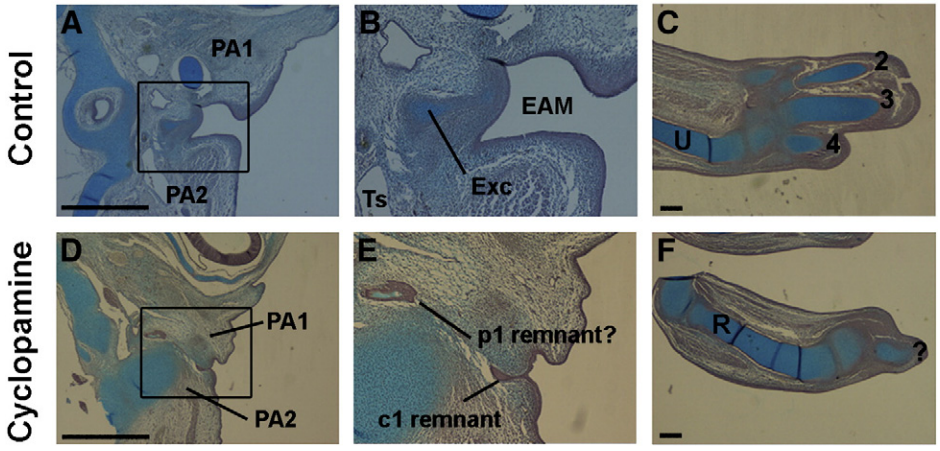

Fig. 9. Hh signalling inhibition by cyclopamine highly impairs the development of the external and middle ear. Embryos were administered with 30 μL of control HbC vehicle (A–C) or cyclopamine (D–F) at HH20–22 and dissected for analysis at E9. Sections in the external ear (A and D) and forelimb (C and F) region were stained with Alcian Blue/Chlorantine Fast Red. (A and B): In the controls, the first cleft developed into the external auditory meatus (EAM), while the first pouch formed the tubotympanic sulcus (Ts), and the second arch ectomesenchyme condensed into extracolumella cartilage (Exc); (C): The control foremimbs show three digits. (D and E): In the cyclopamine-treated embryos, the first cleft failed to invaginate and form the external ear canal, and no recognisable tubotympanic structure and middle ear cartilage are recognisable; (F): Only one digit is recognisable in the forelimbs of the cyclopamine-exposed embryos. PA = pharyngeal arch, U = ulna, R = radius. Scale-bars represent 1000 μm in (A and D) and 100 μm in (C and F).

and grew the embryos up to E9. At this time point, control embryos had well-developed external ear canals, derived from the invagination of the first cleft (Fig. 9B). In the cyclopamine treated embryos, however, the ear canal was often missing or severely reduced in size (Fig. 9E, 6/9). These embryos also showed severe limb defects, as would be expected from loss of *Shh* signalling (Fig. 9C and F). On section, the first arch cleft and pouch could be observed at a distance from each other, the cleft forming a pocket of tissue, but no ectopic parathyroids were identified in any of the embryos (9/9).

Discussion

We show here a striking relationship between the expression of *Gcm2* and low or no *Shh* signalling in the pharyngeal arches of mouse, chick and zebrafish. In the chick and zebrafish we observed no evidence of any *Shh* signalling in the *Gcm2* positive domain, while in the mouse very weak *Ptc1* expression was evident, agreeing with previous observations (Moore-Scott and Manley, 2005). It is possible that very low levels of *Shh* signalling were also present in the chick and zebrafish *Gcm2* positive domain, but were undetectable by in situ hybridisation.

Interestingly, in chick embryos, transient expression of *Gcm2* is observed in the second pouch, while such expression has not been reported in the mouse. This appears to correlate with a change in *Hoxa3* expression during pharyngeal arch formation, as at HH24 *Hoxa3* expression expands anteriorly to encompass the second pouch at the same time as the transient second pouch expression of *Gcm2* is observed. In zebrafish, the expression of *Gcm2* is also closely linked to expression of *Hoxa3* and *Hoxb3* in the pharyngeal arch epithelium from the onset of *Gcm2* activation (Hogan et al., 2004). Reminiscent of the *Hoxa3*−/− mice, the *Hoxa3;Hoxb3* double morphants exhibit a loss of *Gcm2* in the gill epithelium (Hogan et al., 2004).

The inhibition of Hh signalling at different developmental stages using *in ovo* cyclopamine injections in the chick revealed that the Hh pathway plays distinct roles over time during parathyroid development (illustrated in Fig. 10).

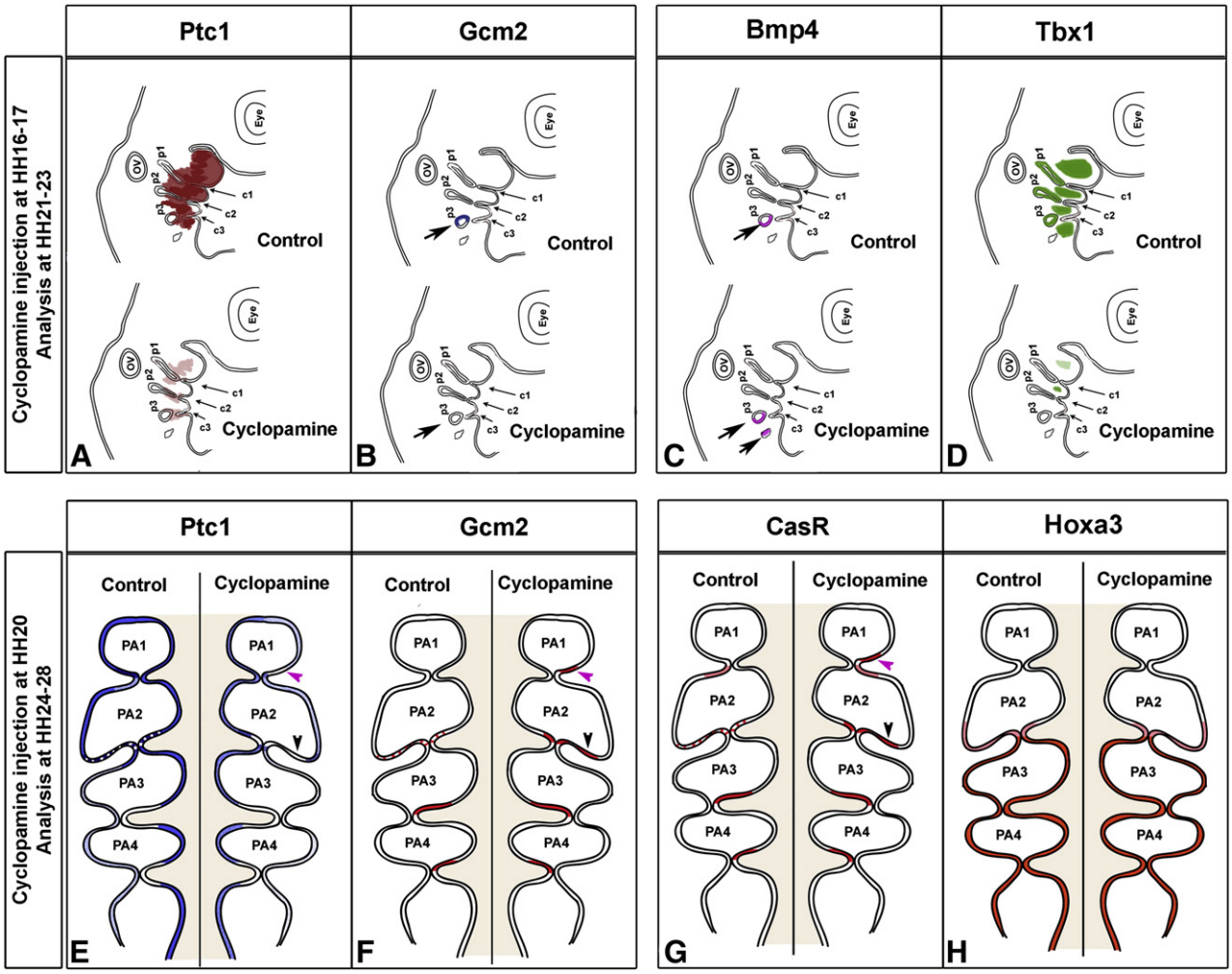

Fig. 10. Effect of Hh signalling inhibition on gene expression in the pharyngeal epithelium. (A–D): Schematic parasagittal views of the pharyngeal region of HH20 chick embryos, illustrating the effect of Hh inhibition at HH16–17 on gene expression. Following cyclopamine exposure at HH16–17 the pharyngeal arches are reduced in size compared to controls. *Ptc1* (A) is decreased throughout the pharyngeal epithelium, including in the anterior part of the third pouch; *Gcm2* (B) is reduced or absent in the anterior aspect of the third pouch (arrow); *Bmp4* (C) is upregulated in the caudal pharyngeal pouches (arrows); *Tbx1* (D) is downregulated in the pharyngeal mesoderm and endoderm, including at the level of the third pouch. (E–H): Schematic frontal views of the pharyngeal region of HH24 chick embryos, illustrating the effects of Hh inhibition at HH20 on gene expression. Only the expression in the pharyngeal epithelium is shown. The pharynx is coloured in light pink. The grade in colour illustrates the intensity of gene expression. (E): Cyclopamine exposure decreases *Ptc1* throughout the pharyngeal epithelium, and more particularly in the anterior part of the first cleft (pink arrowhead) and posterior second arch epithelium (black arrowhead). (F): Hh inhibition ectopically activates *Gcm2* in the anterior first cleft (pink arrowhead) and posterior second arch (black arrowhead). The zones of *Gcm2* misexpression coincide with those of reduced *Ptc1* (arrowheads in E, F). (G): Downregulation of Hh leads to ectopic *CasR* activation in the epithelium of the rostral first cleft and posterior second arch (pink and black arrowheads respectively). Such expression co-localises with ectopic *Gcm2* (compare F and G). (H): At HH24 in the controls, *Hoxa3* is present in the pharyngeal epithelium of the third and fourth arches, including in the pouches, as well as in the posterior second arch epithelium. Cyclopamine at HH20 has no effect on *Hoxa3*. PA = pharyngeal arches, p = pharyngeal pouches, c = pharyngeal cleft, OV = otic vesicle.

From around HH17 to HH20, Hh signalling is involved in setting up the initial pattern of the pharyngeal arches. Disturbances in *Shh* signalling at this stage lead to defects in patterning of the arches, the third arch is perturbed, and there is no induction of *Gcm2*. However, antagonising the Hh pathway after this stage, once arch pattern is established, has no effect on the endogenous *Gcm2* expression. Strikingly, however, loss of *Shh* signalling at later stages led to ectopic *Gcm2* in the anterior first cleft as well as in the anterior second pouch or cleft. *Ptc1* ISH on serial sections confirmed that the aberrant expression of *Gcm2* observed in the drug-treated embryos were associated with a local decrease in *Ptc1* expression. Moreover, in the occasional control embryos that displayed *Gcm2* in the posterior second arch epithelial margin, *Ptc1* expression was found restricted from the limited area of the epithelium transcribing *Gcm2*. All together, these data support the idea that the presence of active Hh signalling from HH21 onwards in the anterior first ectodermal cleft and posterior second arch epithelium represses *Gcm2*, restricting the development of parathyroids to the caudal pouches.

This may represent a common mechanism for restricting the development of endodermally derived primordia. In the context of thyroid and pancreas development, as in that of parathyroid genesis, *Shh* is restricted from the endoderm-derived organ primordia, whereas it is present throughout the surrounding endoderm (Ahlgren et al., 1997; Apelqvist et al., 1997; Fagman et al., 2004; Hebrok et al., 1998). Interestingly, in the *Shh*−/− mutants, ectopic thyroid-specific protein expression was detected in the trachea epithelium, which normally expresses *Shh* (Fagman et al., 2004). Similarly, ectopic pancreatic specific markers were evidenced in the stomach and duodenum primordium of chicken embryos injected with cyclopamine (Kim and Melton, 1998). Thus, in developing tetrapods, Hh signalling may be required in the endoderm adjacent to developing primordia in order to suppress the emergence of ectopic organ derivatives. In the case of the parathyroids, ectopic *Gcm2* was not found in the endoderm adjacent to the anterior third pouch but in some epithelia that, at least for the first cleft, are ectodermal. Our expression analysis showed that the anterior first cleft and posterior second arch epithelium, as the anterior third and fourth pouches, display *Fgf8* and *Pax1* expressions whereas they do not express *Bmp4*. Thus these epithelia share common characteristics with the anterior third or fourth pouches that allow *Gcm2* activation in the absence of Hh signalling.

No changes in *Hoxa3* expression were noted in the Hh-depleted animals, implying that the presence of ectopic *Gcm2* expression in the anterior arch epithelium of the latter does not reflect a change in the pharyngeal arch identity. Upregulation of *Gcm2* after cyclopamine-treatment, was associated with upregulation of *CasR*. Mouse *CasR* does not require *Gcm2* for its activation in the pharyngeal pouches (Liu et al., 2007). The *CasR* gene, however, includes a *Gcm2* response element in each of its two promoters, and *in vitro* transfection assays have shown that *Gcm2* is able to upregulate *CasR* in parathyroid cells (Canaff et al., 2009). In the context of Hh inhibition, ectopic *Gcm2* may therefore directly induce *CasR* misexpression in the pharyngeal epithelium. Although we saw ectopic *CasR* associated with the ectopic *Gcm2*, no ectopic expression of *PTH* was observed after cyclopamine treatment. *PTH* expression comes on relatively late during chick parathyroid development and the lack of ectopic expression indicates that although ectopic parathyroids might have been initiated in the rostral arches they were unable to undergo differentiation to form parathyroid tissue. This agrees with the fact that no ectopic parathyroids were observed at later stages. It is perhaps not surprising that the ectopic first arch *Gcm2*/*CasR* positive tissue was unable to form a normal parathyroid that can migrate as many of the factors necessary for parathyroid migration or late differentiation, such as *Hoxd3* and *Hoxb3* are expressed in the posterior pharyngeal pouches but are missing in the anterior arch epithelium (Manley and Capecchi, 1998).

The above data converge towards a model in which at HH21–24, the absence of Hh signalling, together with the presence of *Fgf8* and *Pax1* and the absence of *Bmp4*, are required in the pharyngeal epithelium to allow expression of *Gcm2*. In mouse and zebrafish, *Hoxa3*/*b3* function is required for *Gcm2* activation or maintenance in the pharyngeal region. Still, in the cyclopamine-treated embryos, the absence of *Hoxa3* from the first cleft *Gcm2* ectopic domain provides evidence that at least under Hh reduction, and in the presence of *Fgf8* and *Pax1*, *Gcm2* in the pharyngeal epithelium does not rely on *Hoxa3*. One possibility for reconciling all these observations is that *Hoxa3* inhibits the Hh pathway in the pharyngeal epithelium. In the third and fourth caudal pouch, the negative regulation of Hh signalling by *Hoxa3* would stop the inhibition of *Gcm2*, whereas in the anterior arch epithelium, the lack of *Hoxa3* would permit Hh driven suppression of this gene. It would be interesting to test this hypothesis by investigating the effects of mis-expressing *Hoxa3* in the chick first cleft on *Gcm2* and *Ptc1*, and by analysing *Ptc1* in the *Hoxa3*−/− mice.

Supplementary materials related to this article can be found online at doi:10.1016/j.ydbio.2011.02.012.

Conflicts of interest

The authors confirm that they have no conflict of interests.

Acknowledgments

This work was funded by an EU Marie Curie Early Stage Career fellowship. Thanks to Nancy Manley for the mouse *Gcm2* probe.

References

Abu-Issa, R., Smyth, G., Smoak, I., Yamamura, K., Meyers, E.N., 2002. Fgf8 is required for pharyngeal arch and cardiovascular development in the mouse. Development 129, 4613–4625.

Ahlgren, U., Pfaff, S.L., Jessell, T.M., Edlund, T., Edlund, H., 1997. Independent requirement for ISL1 in formation of pancreatic mesenchyme and islet cells. Nature 385, 257–260.

Apelqvist, A., Ahlgren, U., Edlund, H., 1997. Sonic hedgehog directs specialised mesoderm differentiation in the intestine and pancreas. Curr. Biol. 7, 801–804.

Canaff, L., Zhou, X., Mosesova, I., Cole, D.E., Hendy, G.N., 2009. Glial cells missing-2 (GCM2) transactivates the calcium-sensing receptor gene: effect of a dominant-negative GCM2 mutant associated with autosomal dominant hypoparathyroidism. Hum. Mutat. 30, 85–92.

Chang, W.J., Horng, J.L., Yan, J.J., Hsiao, C.D., Hwang, P.P., 2009. The transcription factor, glial cell missing 2, is involved in differentiation and functional regulation of H+-ATPase-rich cells in zebrafish (*Danio rerio*). Am. J. Physiol. Regul. Integr. Comp. Physiol. 296, R1192–R1201.

Clay, H., Ramakrishnan, L., 2005. Multiplex fluorescent in situ hybridization in zebrafish embryos using tyramide signal amplification. Zebrafish 2, 105–111.

Cordero, D., Marcucio, R., Hu, D., Gaffield, W., Tapadia, M., Helms, J.A., 2004. Temporal perturbations in sonic hedgehog signaling elicit the spectrum of holoprosencephaly phenotypes. J. Clin. Invest. 114, 485–494.

Denkers, N., Garcia-Villalba, P., Rodesch, C.K., Nielson, K.R., Mauch, T.J., 2004. FISHing for chick genes: triple-label whole-mount fluorescence in situ hybridization detects simultaneous and overlapping gene expression in avian embryos. Dev. Dyn. 229, 651–657.

Echelard, Y., Epstein, D.J., St-Jacques, B., Shen, L., Mohler, J., McMahon, J.A., McMahon, A.P., 1993. Sonic hedgehog, a member of a family of putative signaling molecules, is implicated in the regulation of CNS polarity. Cell 75, 1417–1430.

Fagman, H., Grande, M., Gritli-Linde, A., Nilsson, M., 2004. Genetic deletion of sonic hedgehog causes hemiagenesis and ectopic development of the thyroid in mouse. Am. J. Pathol. 164, 1865–1872.

Frank, D.U., Fotheringham, L.K., Brewer, J.A., Muglia, L.J., Tristani-Firouzi, M., Capecchi, M.R., Moon, A.M., 2002. An Fgf8 mouse mutant phenocopies human 22q11 deletion syndrome. Development 129, 4591–4603.

Goodrich, L.V., Johnson, R.L., Milenkovic, L., McMahon, J.A., Scott, M.P., 1996. Conservation of the hedgehog/patched signaling pathway from flies to mice: induction of a mouse patched gene by hedgehog. Genes Dev. 10, 301–312.

Gordon, J., Bennett, A.R., Blackburn, C.C., Manley, N.R., 2001. Gcm2 and Foxn1 mark early parathyroid- and thymus-specific domains in the developing third pharyngeal pouch. Mech. Dev. 103, 141–143.

Gordon, J., Patel, S.R., Mishina, Y., Manley, N.R., 2010. Evidence for an early role for BMP4 signaling in thymus and parathyroid morphogenesis. Dev. Biol. 339, 141–154.

Grevellec, A., Tucker, A.S., 2010. The pharyngeal pouches and clefts: Development, evolution, structure and derivatives. Semin. Cell. Dev. Biol. 21, 325–332.

Hahn, H., Christiansen, J., Wicking, C., Zaphiropoulos, P.G., Chidambaram, A., Gerrard, B., Vorechovsky, I., Bale, A.E., Toftgard, R., Dean, M., Wainwright, B., 1996. A mammalian patched homolog is expressed in target tissues of sonic hedgehog and maps to a region associated with developmental abnormalities. J. Biol. Chem. 271, 12125–12128.

Hamburger, V., Hamilton, H.L., 1992. A series of normal stages in the development of the chick embryo. 1951. Dev. Dyn. 195, 231–272.

Hanaoka, R., Ohmori, Y., Uyemura, K., Hosoya, T., Hotta, Y., Shirao, T., Okamoto, H., 2004. Zebrafish gcmb is required for pharyngeal cartilage formation. Mech. Dev. 121, 1235–1247.

Hebrok, M., Kim, S.K., Melton, D.A., 1998. Notochord repression of endodermal Sonic hedgehog permits pancreas development. Genes Dev. 12, 1705–1713.

Hogan, B.M., Hunter, M.P., Oates, A.C., Crowhurst, M.O., Hall, N.E., Heath, J.K., Prince, V.E., Lieschke, G.J., 2004. Zebrafish gcm2 is required for gill filament budding from pharyngeal ectoderm. Dev. Biol. 276, 508–522.

Hunt, P., Clarke, J.D., Buxton, P., Ferretti, P., Thorogood, P., 1998. Stability and plasticity of neural crest patterning and branchial arch Hox code after extensive cephalic crest rotation. Dev. Biol. 198, 82–104.

Hunt, P., Krumlauf, R., 1992. Hox codes and positional specification in vertebrate embryonic axes. Annu. Rev. Cell Biol. 8, 227–256.

Kim, S.K., Melton, D.A., 1998. Pancreas development is promoted by cyclopamine, a hedgehog signaling inhibitor. Proc. Natl Acad. Sci. USA 95, 13036–13041.

Krauss, S., Concordet, J.P., Ingham, P.W., 1993. A functionally conserved homolog of the *Drosophila* segment polarity gene hh is expressed in tissues with polarizing activity in zebrafish embryos. Cell 75, 1431–1444.

Lewis, K.E., Concordet, J.P., Ingham, P.W., 1999. Characterisation of a second patched gene in the zebrafish *Danio rerio* and the differential response of patched genes to hedgehog signalling. Dev. Biol. 208, 14–29.

Liu, Z., Yu, S., Manley, N.R., 2007. Gcm2 is required for the differentiation and survival of parathyroid precursor cells in the parathyroid/thymus primordia. Dev. Biol. 305, 333–346.

Manley, N.R., Capecchi, M.R., 1995. The role of Hoxa-3 in mouse thymus and thyroid development. Development 121, 1989–2003.

Manley, N.R., Capecchi, M.R., 1998. Hox group 3 paralogs regulate the development and migration of the thymus, thyroid, and parathyroid glands. Dev. Biol. 195, 1–15.

Manley, N.R., Selleri, L., Brendolan, A., Gordon, J., Cleary, M.L., 2004. Abnormalities of caudal pharyngeal pouch development in Pbx1 knockout mice mimic loss of Hox3 paralogs. Dev. Biol. 276, 301–312.

Moore-Scott, B.A., Manley, N.R., 2005. Differential expression of Sonic hedgehog along the anterior–posterior axis regulates patterning of pharyngeal pouch endoderm and pharyngeal endoderm-derived organs. Dev. Biol. 278, 323–335.

Mootoosamy, R.C., Dietrich, S., 2002. Distinct regulatory cascades for head and trunk myogenesis. Development 129, 573–583.

Okabe, M., Graham, A., 2004. The origin of the parathyroid gland. Proc. Natl Acad. Sci. USA 101, 17716–17719.

Patel, S.R., Gordon, J., Mahbub, F., Blackburn, C.C., Manley, N.R., 2006. Bmp4 and Noggin expression during early thymus and parathyroid organogenesis. Gene Expr. Patterns 6, 794–799.

Platt, K.A., Michaud, J., Joyner, A.L., 1997. Expression of the mouse Gli and Ptc genes is adjacent to embryonic sources of hedgehog signals suggesting a conservation of pathways between flies and mice. Mech. Dev. 62, 121–135.

Potts, J.T., 2005. Parathyroid hormone: past and present. J. Endocrinol. 187, 311–325.

Su, D., Ellis, S., Napier, A., Lee, K., Manley, N.R., 2001. Hoxa3 and pax1 regulate epithelial cell death and proliferation during thymus and parathyroid organogenesis. Dev. Biol. 236, 316–329.

Vitelli, F., Taddei, I., Morishima, M., Meyers, E.N., Lindsay, E.A., Baldini, A., 2002. A genetic link between Tbx1 and fibroblast growth factor signaling. Development 129, 4605–4611.

Wallin, J., Eibel, H., Neubuser, A., Wilting, J., Koseki, H., Balling, R., 1996. Pax1 is expressed during development of the thymus epithelium and is required for normal T-cell maturation. Development 122, 23–30.

Washington Smoak, I., Byrd, N.A., Abu-Issa, R., Goddeeris, M.M., Anderson, R., Morris, J., Yamamura, K., Klingensmith, J., Meyers, E.N., 2005. Sonic hedgehog is required for cardiac outflow tract and neural crest cell development. Dev. Biol. 283, 357–372.

Welten, M.C., de Haan, S.B., van den Boogert, N., Noordermeer, J.N., Lamers, G.E., Spaink, H.P., Meijer, A.H., Verbeek, F.J., 2006. Zebrafish: fluorescent in situ hybridization protocol and three-dimensional imaging of gene expression patterns. Zebrafish 3, 465–476.